

Supplementary Materials

Self-assembled Nanomaterials Based on Complementary Sn(IV) and Zn(II)-porphyrins, and Their Photocatalytic Degradation for Rhodamine B Dye

Nirmal Kumar Shee and Hee-Joon Kim*

*Department of Applied Chemistry, Kumoh National Institute of Technology
61 Daehak-ro, Gumi 39177, Republic of Korea*

List of contents:

Figure S1. ^1H NMR spectrum of *meso*-5-(4-hydroxyphenyl)-10,15,20-tris(phenyl)porphyrin **H₂L¹** in CDCl_3 .

Figure S2. ^1H NMR spectrum of *meso*-5-(4-hydroxyphenyl)-10,15,20-tris(4-methylphenyl)porphyrin **H₂L²** in CDCl_3 .

Figure S3. ^1H NMR spectrum of *meso*-5-(4-hydroxyphenyl)-10,15,20-tris(4-*tert*-butylphenyl)porphyrin **H₂L³** in CDCl_3 .

Figure S4. ^1H NMR spectrum of *meso*-5-(4-hydroxyphenyl)-10,15,20-tris(4-methoxyphenyl)porphyrin **H₂L⁴** in CDCl_3 .

Figure S5. ^1H NMR spectrum of *meso*-5-(4-hydroxyphenyl)-10,15,20-tris(4-chlorophenyl)porphyrin **H₂L⁵** in CDCl_3 .

Figure S6. ^1H NMR spectrum of *meso*-5-(4-hydroxyphenyl)-10,15,20-tris(4-nitrophenyl)porphyrin **H₂L⁶** in CDCl_3 .

Figure S7. ^1H NMR spectrum of *meso*-5-(4-hydroxyphenyl)-10,15,20-tris(phenyl)porphyrinato)zinc(II) **ZnL¹** in DMSO- d_6 .

Figure S8. ^1H NMR spectrum of *meso*-5-(4-hydroxyphenyl)-10,15,20-tris(4-methylphenyl)porphyrinato)zinc(II) **ZnL²** in DMSO- d_6 .

Figure S9. ^1H NMR spectrum of *meso*-5-(4-hydroxyphenyl)-10,15,20-tris(4-*tert*-butylphenyl)porphyrinato)zinc(II) **ZnL³** in DMSO- d_6 .

Figure S10. ^1H NMR spectrum of *meso*-5-(4-hydroxyphenyl)-10,15,20-tris(4-methoxyphenyl)porphyrinato)zinc(II) **ZnL⁴** in DMSO- d_6 .

Figure S11. ^1H NMR spectrum of *meso*-5-(4-hydroxyphenyl)-10,15,20-tris(4-chlorophenyl)porphyrinato)zinc(II) **ZnL⁵** in DMSO- d_6 .

Figure S12. ^1H NMR spectrum of *meso*-5-(4-hydroxyphenyl)-10,15,20-tris(4-nitrophenyl)porphyrinato)zinc(II) **ZnL⁶** in DMSO- d_6 .

Figure S13. ^1H NMR spectrum of triad **1** in DMSO- d_6 .

Figure S14. ^1H NMR spectrum of triad **2** in DMSO- d_6 .

Figure S15. ^1H NMR spectrum of triad **3** in DMSO- d_6 .

Figure S16. ^1H NMR spectrum of triad **4** in DMSO- d_6 .

Figure S17. ^1H NMR spectrum of triad **5** in DMSO- d_6 .

Figure S18. ^1H NMR spectrum of triad **6** in DMSO- d_6 .

Figure S19. ESI-MS spectrum of triad **1**.

Figure S20. ESI-MS spectrum of triad **2**.

Figure S21. ESI-MS spectrum of triad **3**.

Figure S22. ESI-MS spectrum of triad **4**.

Figure S23. ESI-MS spectrum of triad **5**.

Figure S24. ESI-MS spectrum of triad **6**.

Figure S25. Lower magnification of FE-SEM images for the assembly patterns of triads: (a) **1**; (b) **2**; (c) **3**; (d) **4**; (e) **5**; (f) **6**.

Figure S26. Absorption spectra of RhB in the presence of nano fibers derived from triad **3** under visible light irradiation.

Figure S27. Kinetics for the photocatalytic degradation of RhB under visible light irradiation of the six triads (**1-6**).

Figure S28. Catalytic cycles (up to 5 cycles) using triad **3** as a photocatalyst for the degradation of RhB.

Figure S29. Schematic representation of the detection of the hydroxyl and superoxide radical anion that were generated during the photodegradation experiments.

Figure S30. UV-visible spectra of coumarin in the presence of triad **3** in water. $\lambda_{\text{ex}} = 325$ nm and light exposure time (30 min).

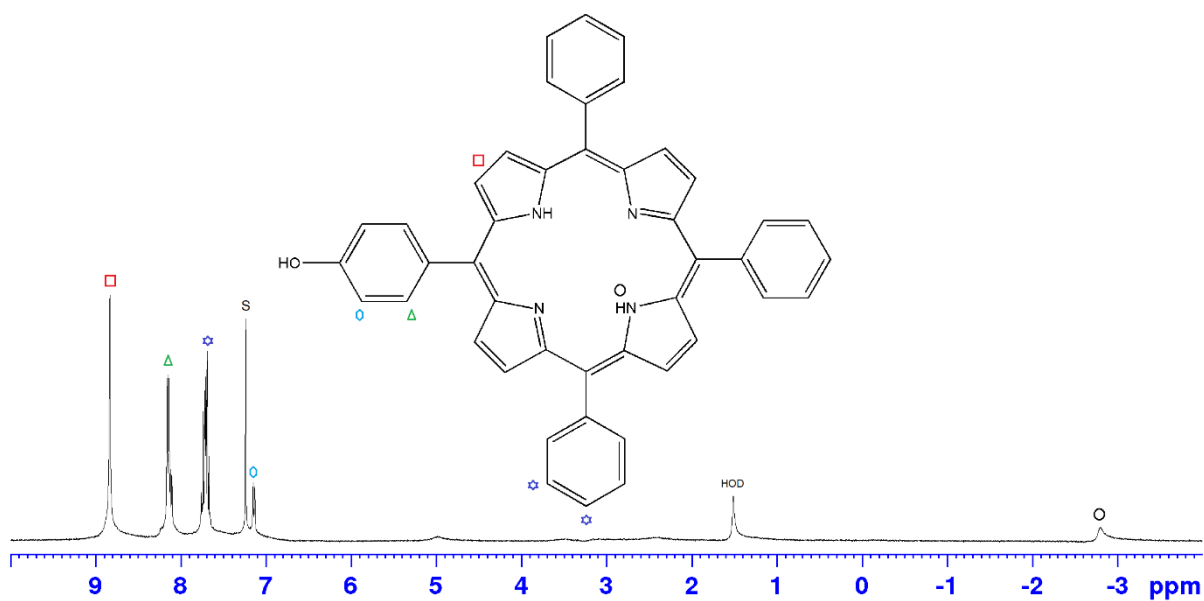


Figure S1. ^1H NMR spectrum of *meso*-5-(4-hydroxyphenyl)-10,15,20-tris(phenyl)porphyrin **H₂L¹** in CDCl_3 .

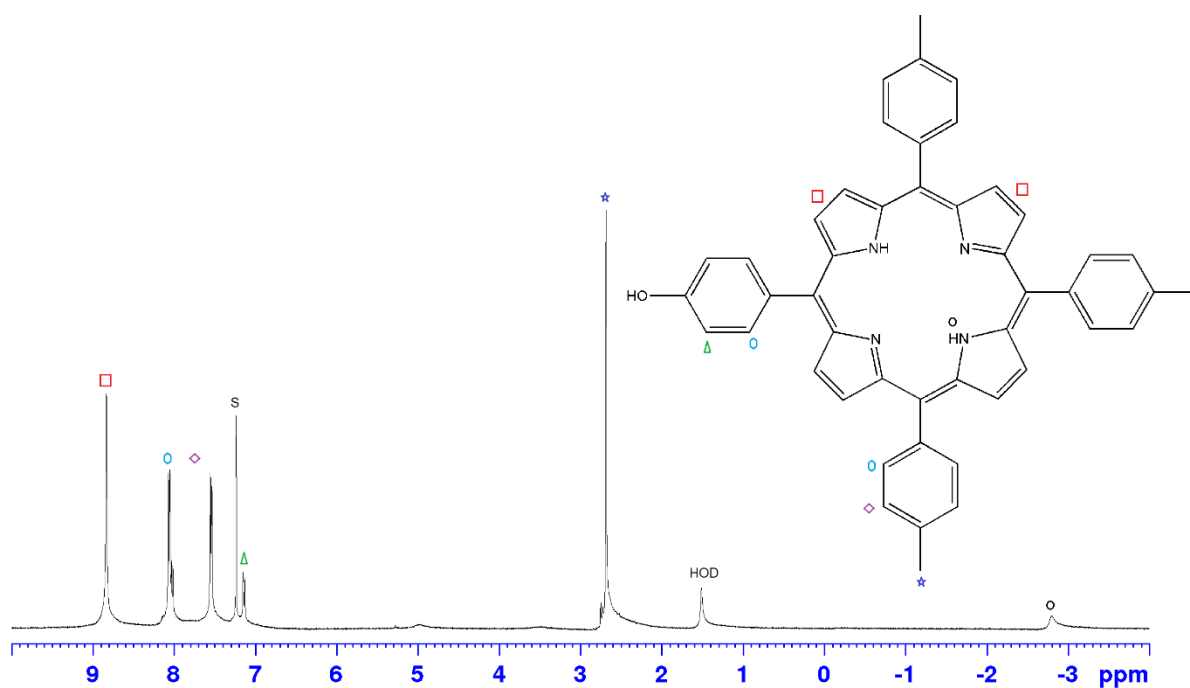


Figure S2. ^1H NMR spectrum of *meso*-5-(4-hydroxyphenyl)-10,15,20-tris(4-methylphenyl)porphyrin **H₂L²** in CDCl_3 .

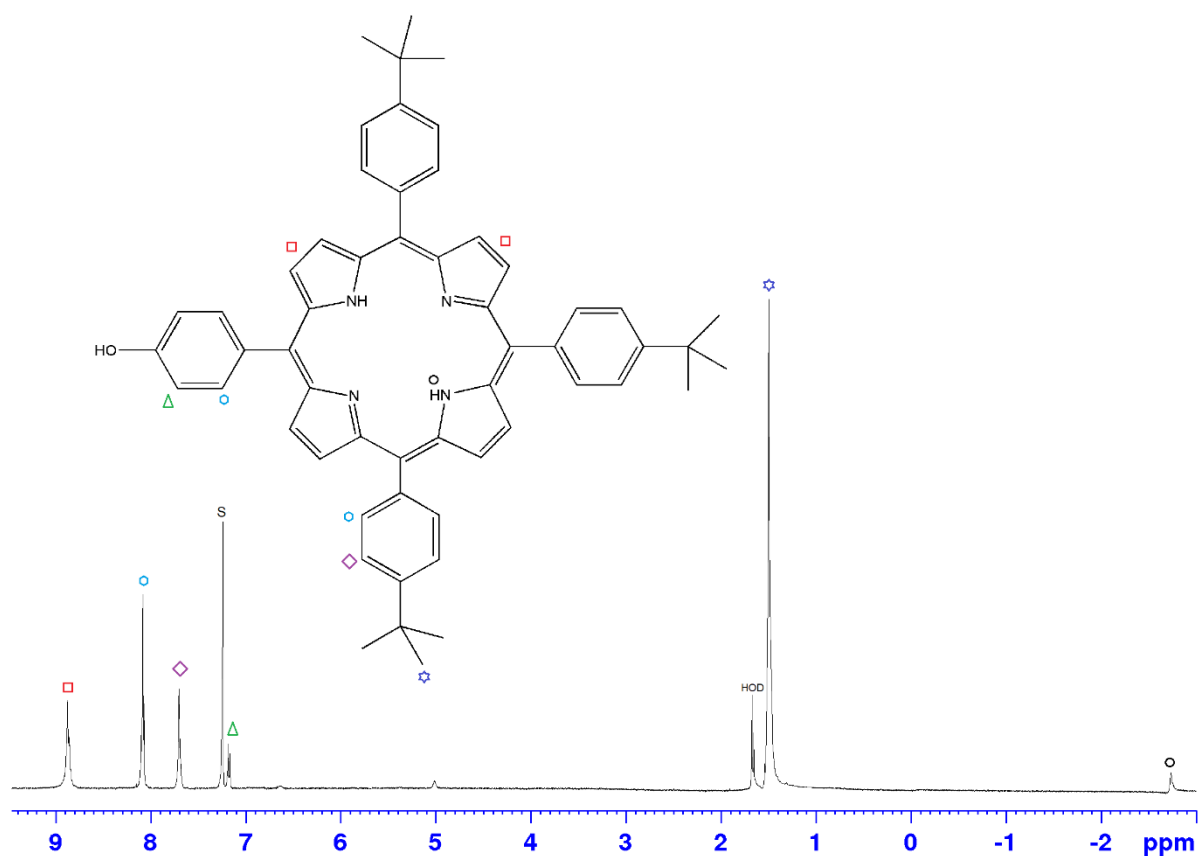


Figure S3. ¹H NMR spectrum of *meso*-5-(4-hydroxyphenyl)-10,15,20-tris(4-*tert*-butylphenyl)porphyrin **H₂L³** in CDCl₃.

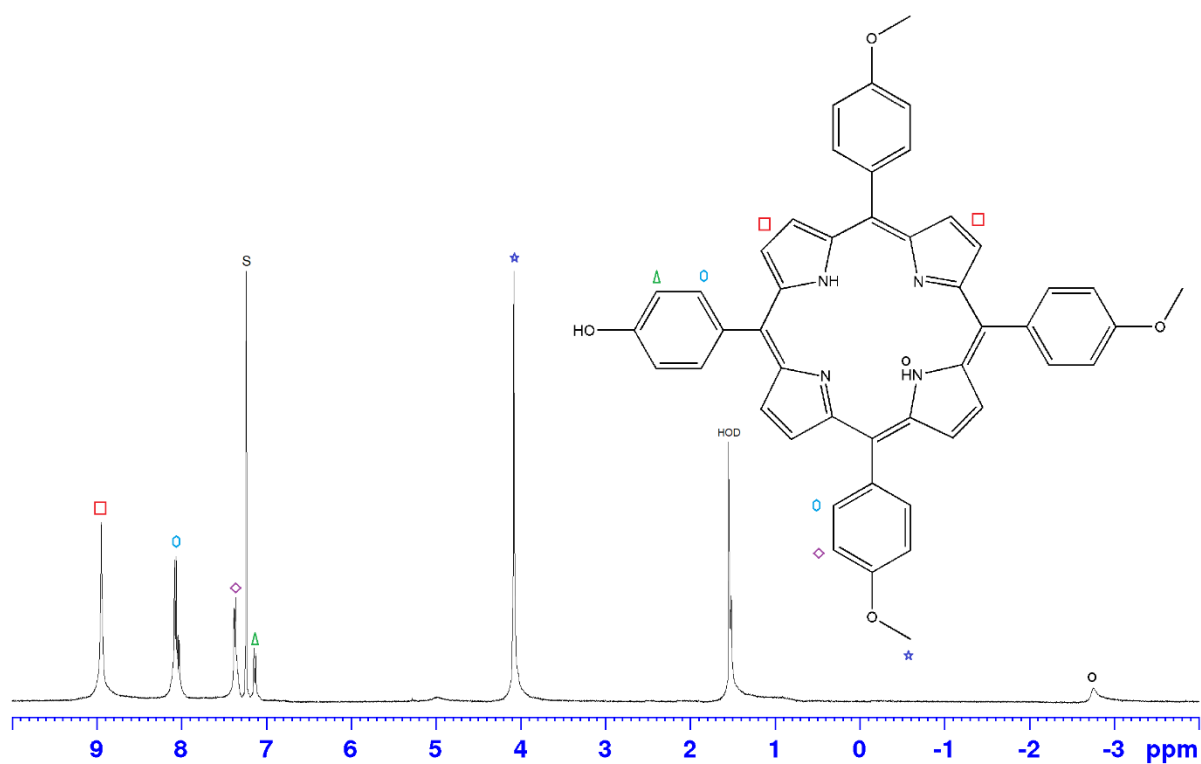


Figure S4. ¹H NMR spectrum of *meso*-5-(4-hydroxyphenyl)-10,15,20-tris(4-methoxyphenyl)porphyrin **H₂L⁴** in CDCl₃.

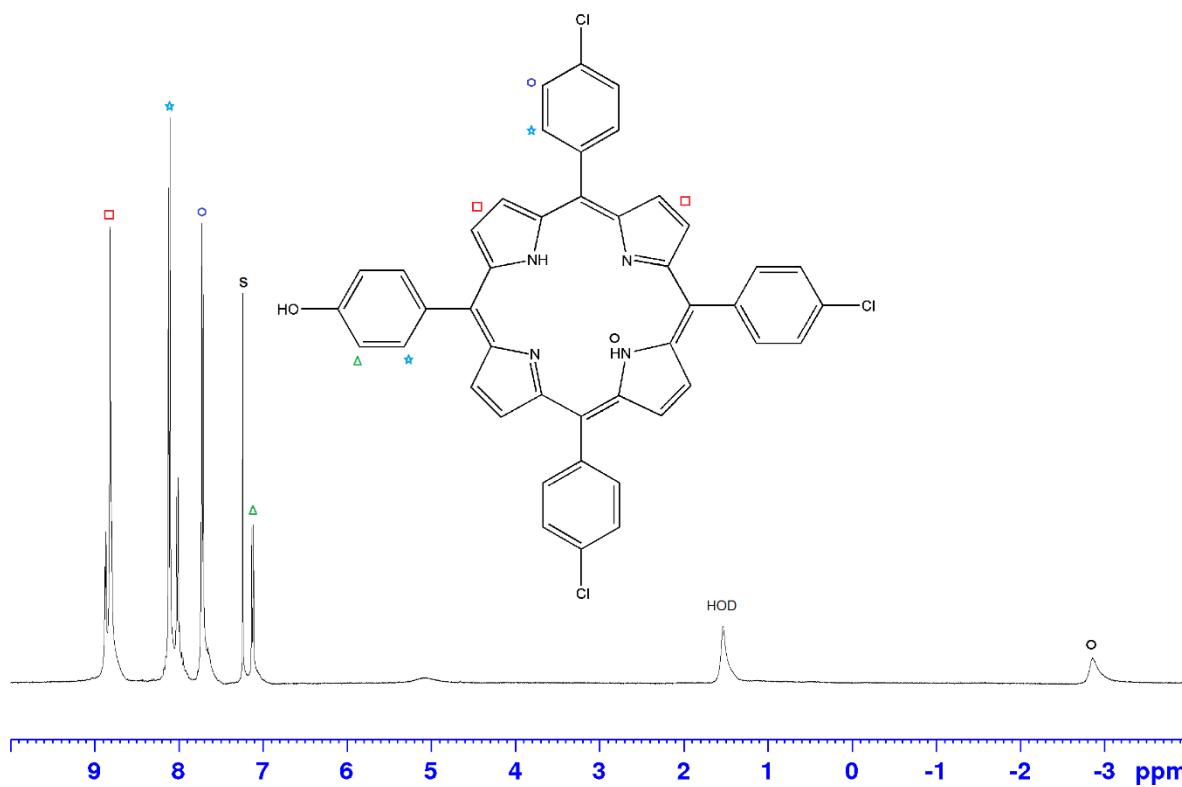


Figure S5. ^1H NMR spectrum of *meso*-5-(4-hydroxyphenyl)-10,15,20-tris(4-chlorophenyl)porphyrin **H₂L⁵** in CDCl_3 .

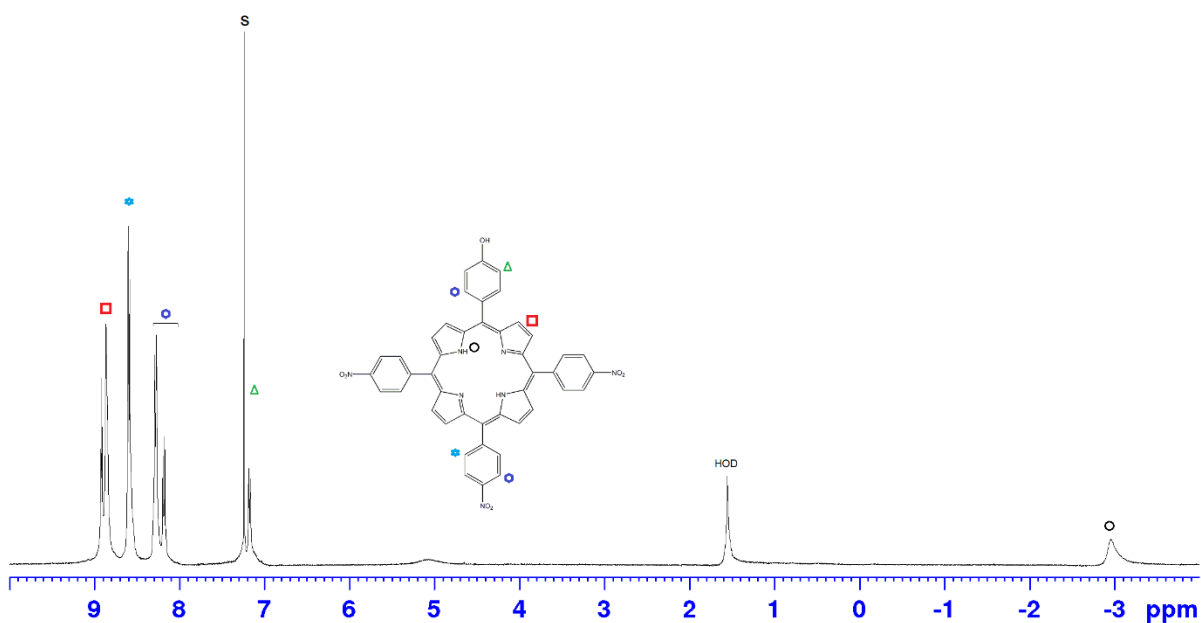


Figure S6. ^1H NMR spectrum of *meso*-5-(4-hydroxyphenyl)-10,15,20-tris(4-nitrophenyl)porphyrin **H₂L⁶** in CDCl_3 .

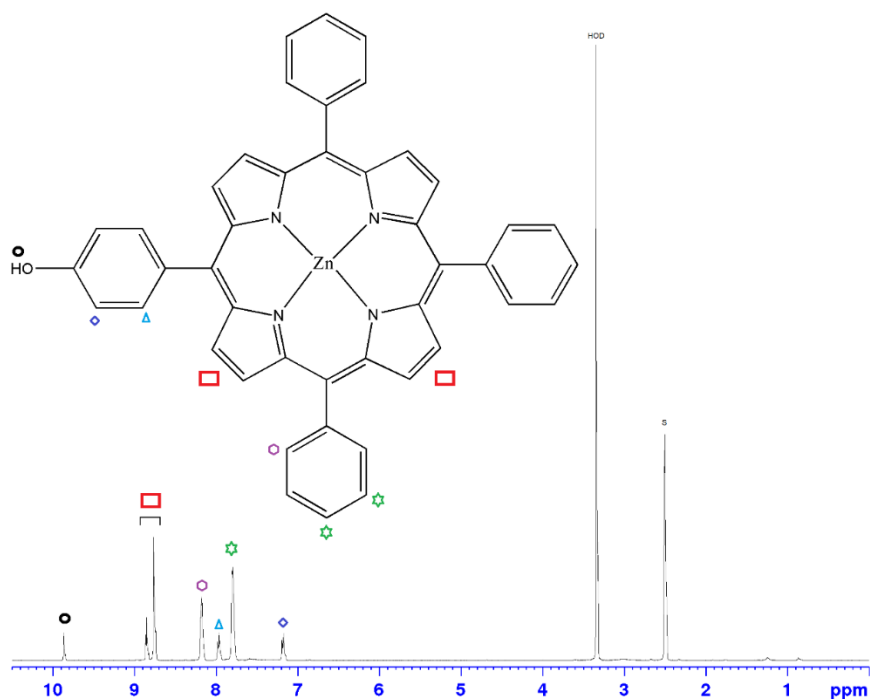


Figure S7. ^1H NMR spectrum of *meso*-5-(4-hydroxyphenyl)-10,15,20-tris(phenyl)porphyrinato)zinc(II) **ZnL¹** in DMSO- d_6 .

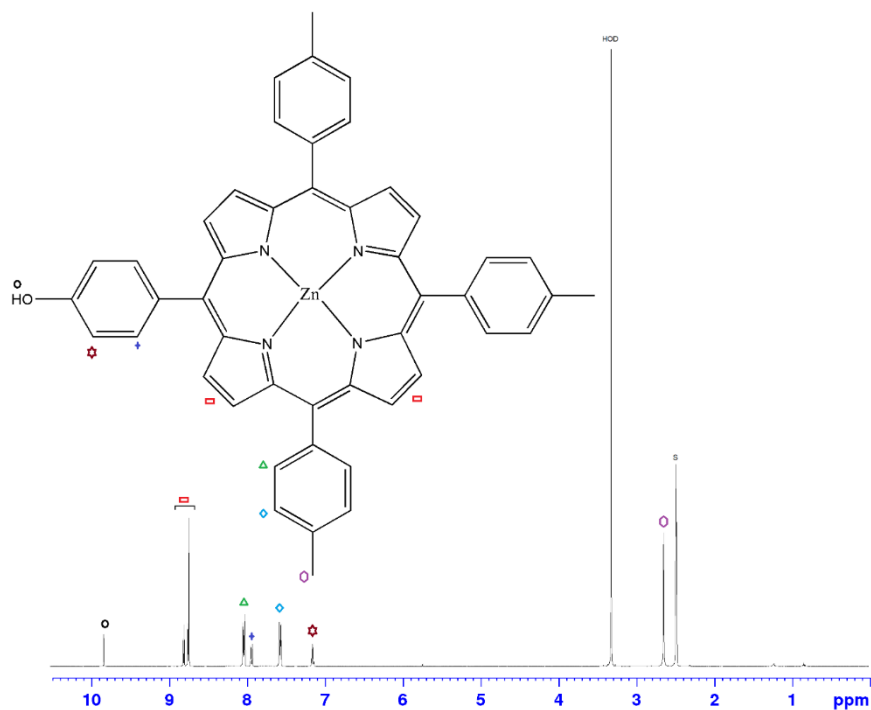


Figure S8. ^1H NMR spectrum of *meso*-5-(4-hydroxyphenyl)-10,15,20-tris(4-methylphenyl)porphyrinato)zinc(II) **ZnL²** in DMSO- d_6 .

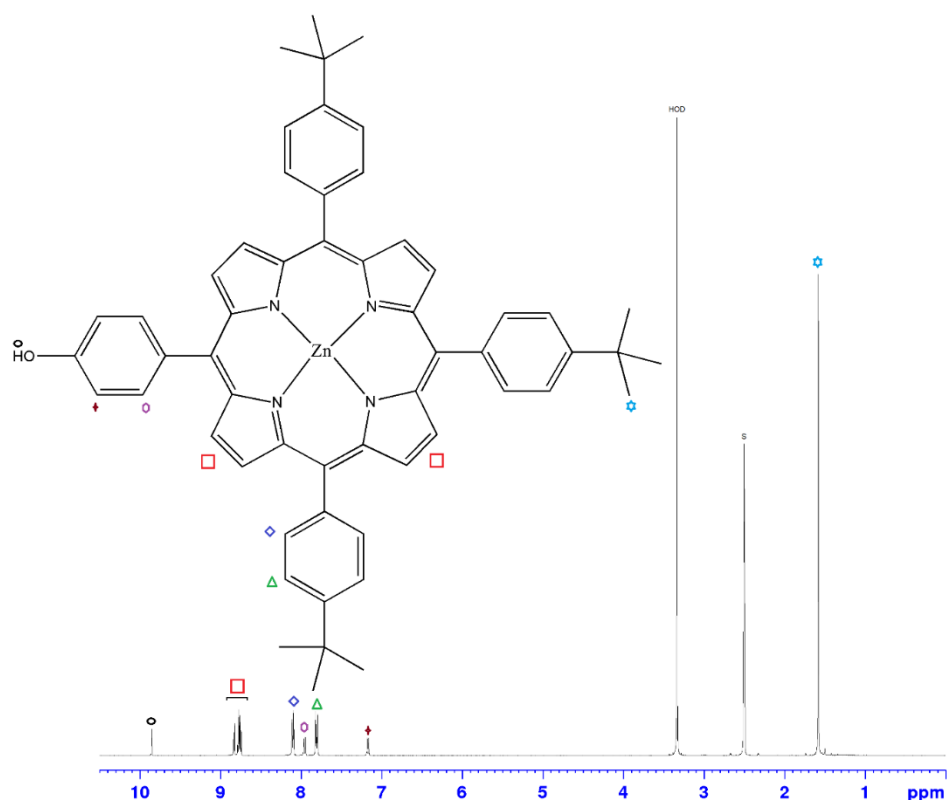


Figure S9. ^1H NMR spectrum of *meso*-5-(4-hydroxyphenyl)-10,15,20-tris(4-*tert*-butylphenyl)porphyrinato)zinc(II) **ZnL³** in DMSO- d_6 .

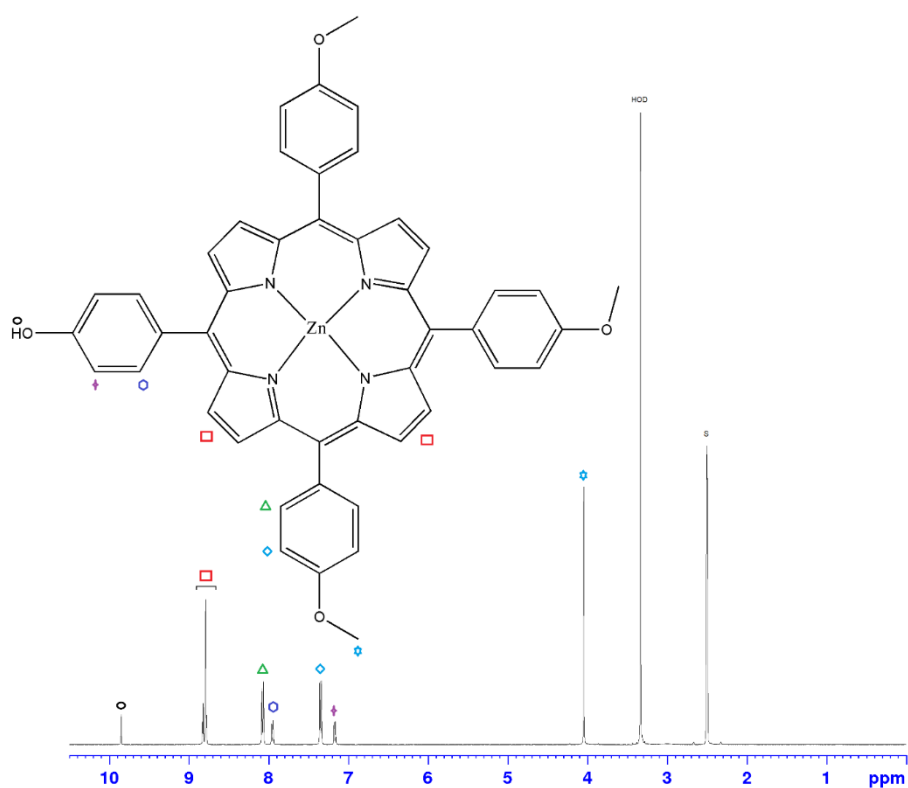


Figure S10. ^1H NMR spectrum of *meso*-5-(4-hydroxyphenyl)-10,15,20-tris(4-methoxyphenyl)porphyrinato)zinc(II) **ZnL⁴** in DMSO- d_6 .

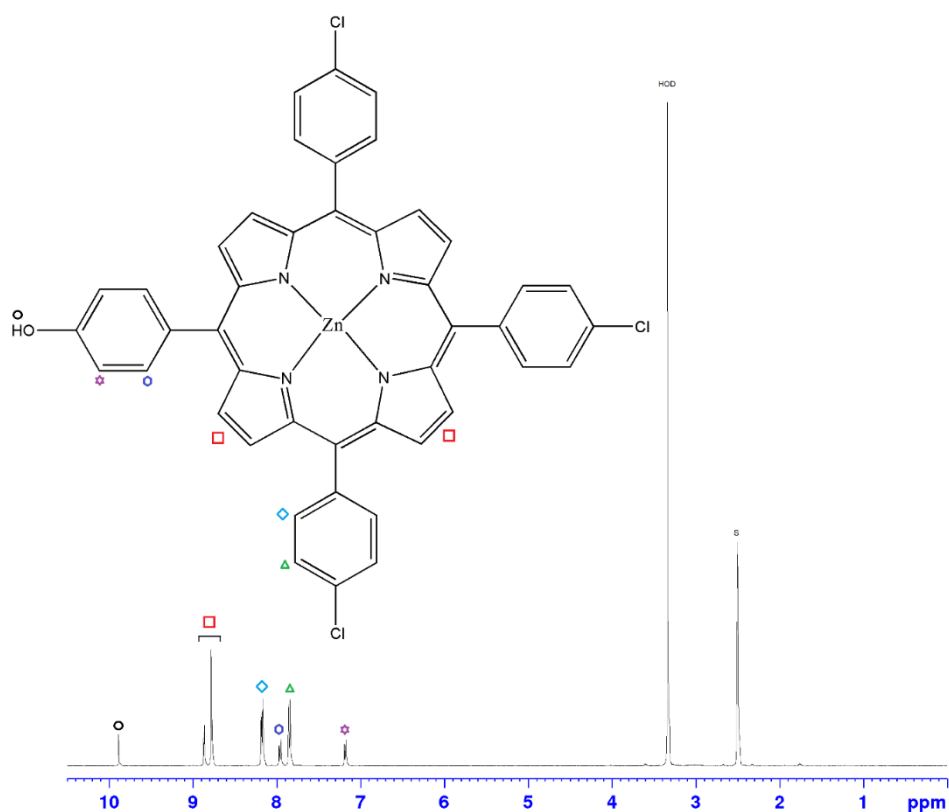


Figure S11. ^1H NMR spectrum of *meso*-5-(4-hydroxyphenyl)-10,15,20-tris(4-chlorophenyl)porphyrinato)zinc(II) **ZnL⁵** in DMSO- d_6 .

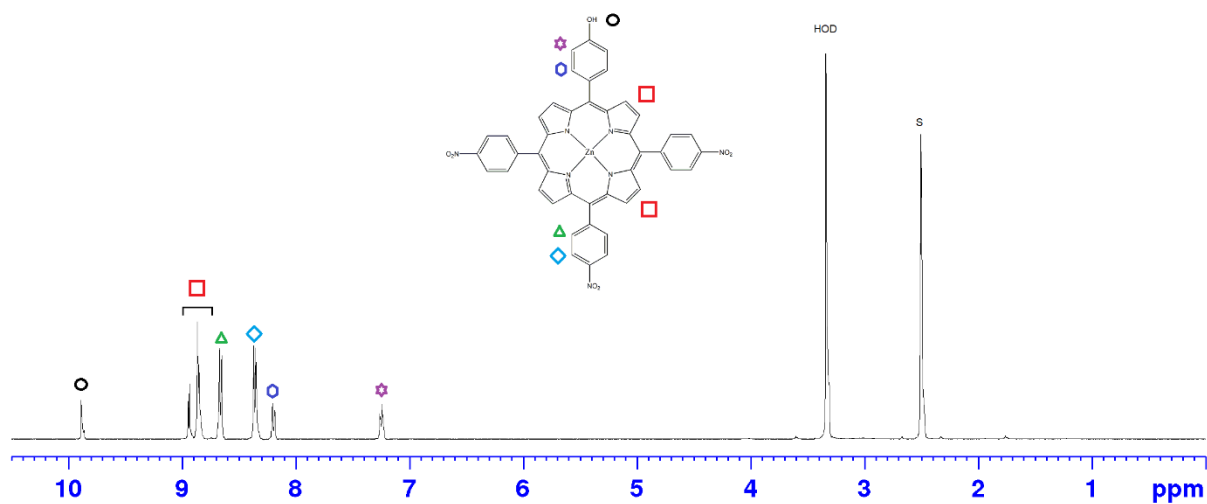


Figure S12. ^1H NMR spectrum of *meso*-5-(4-hydroxyphenyl)-10,15,20-tris(4-nitrophenyl)porphyrinato)zinc(II) **ZnL⁶** in DMSO- d_6 .

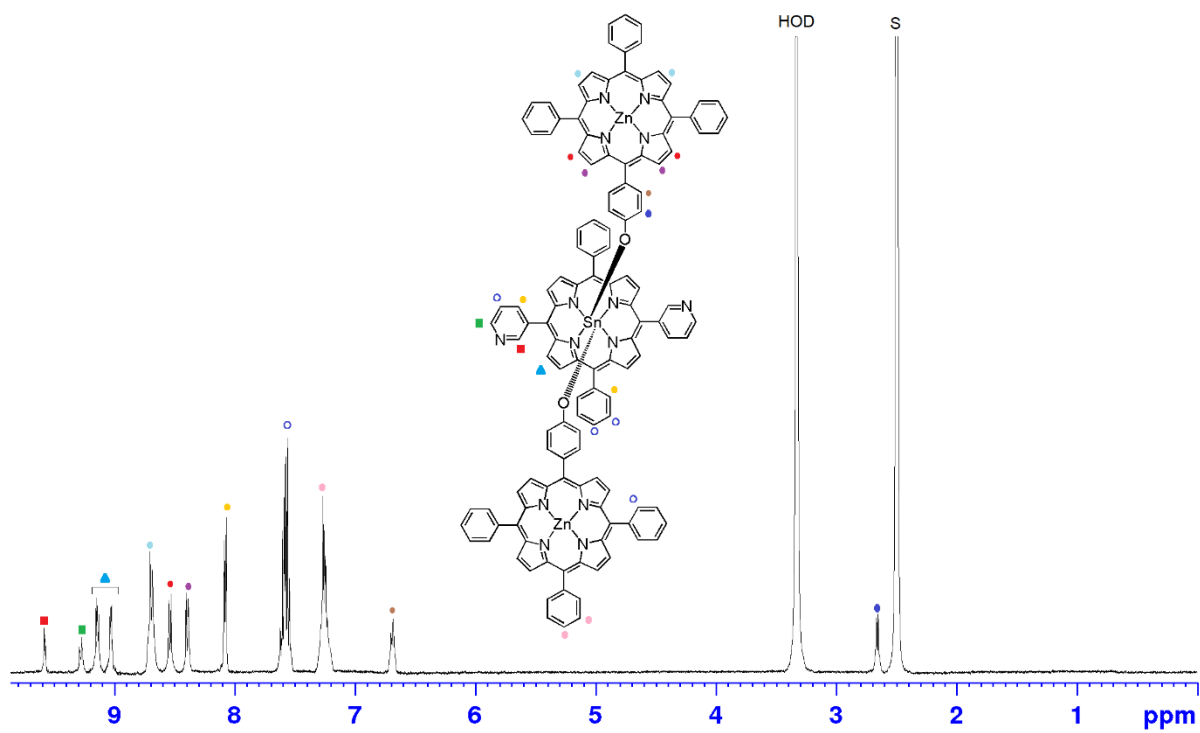


Figure S13. ^1H NMR spectrum of triad **1** in DMSO-d_6 .

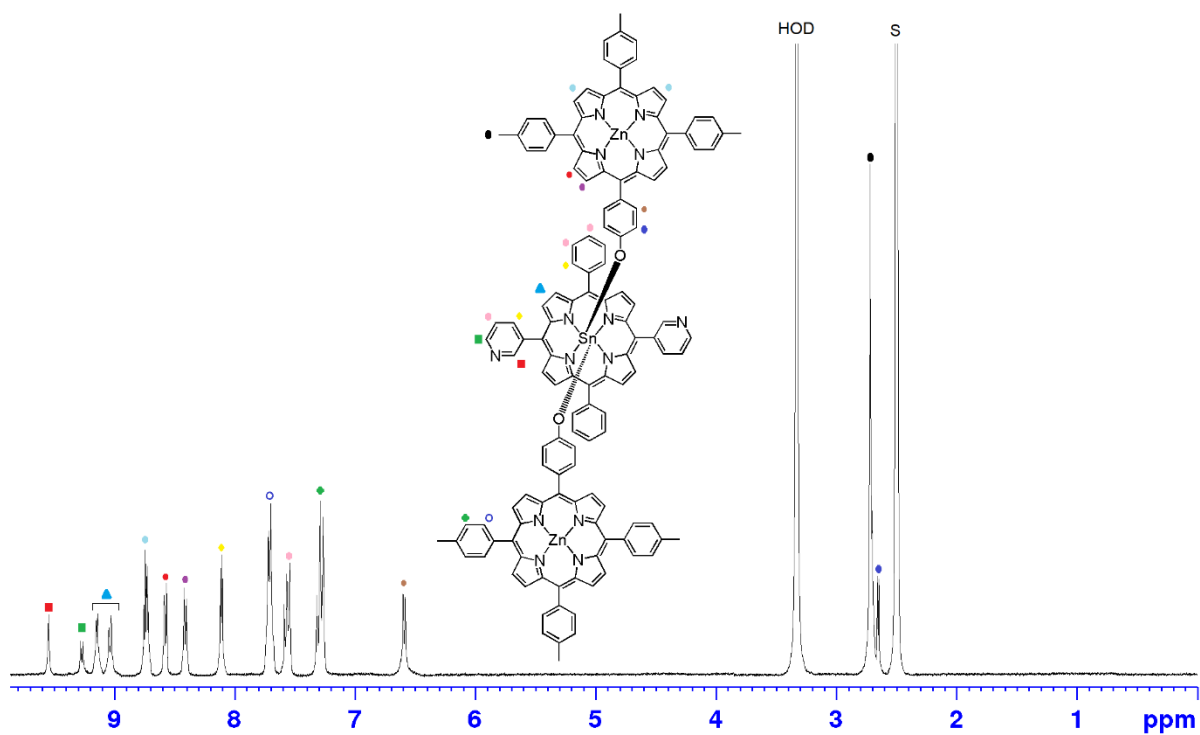


Figure S14. ^1H NMR spectrum of triad **2** in DMSO-d_6 .

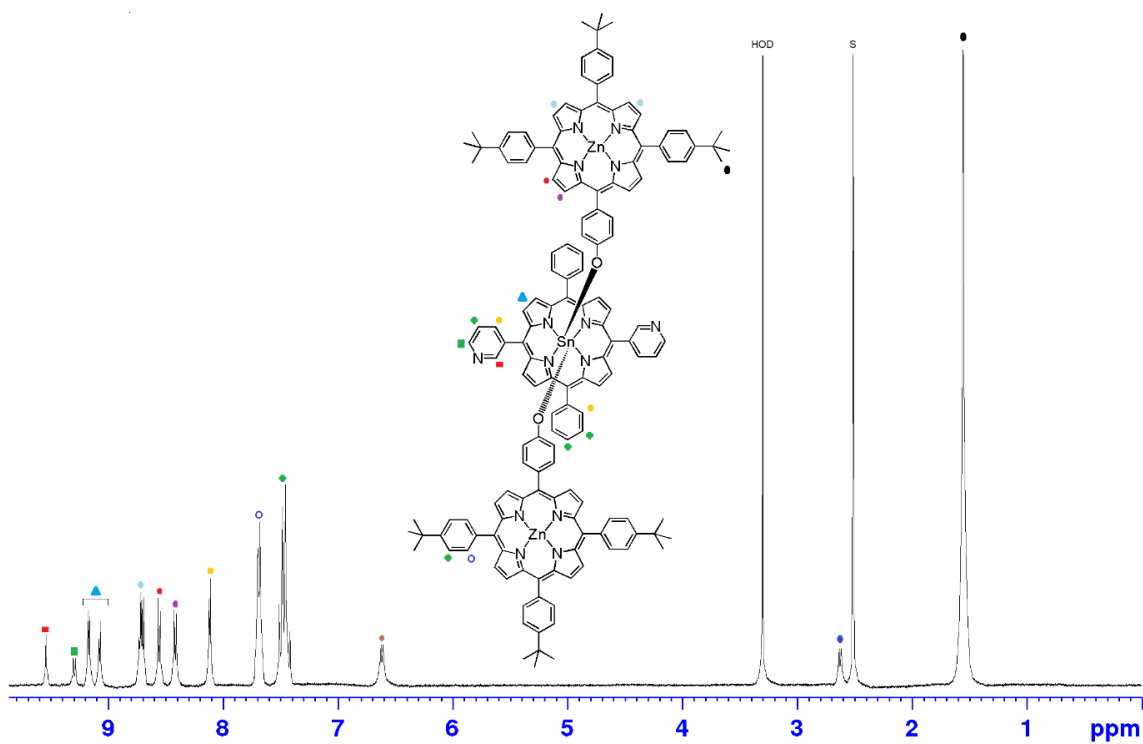


Figure S15. ¹H NMR spectrum of triad **3** in DMSO-d₆.

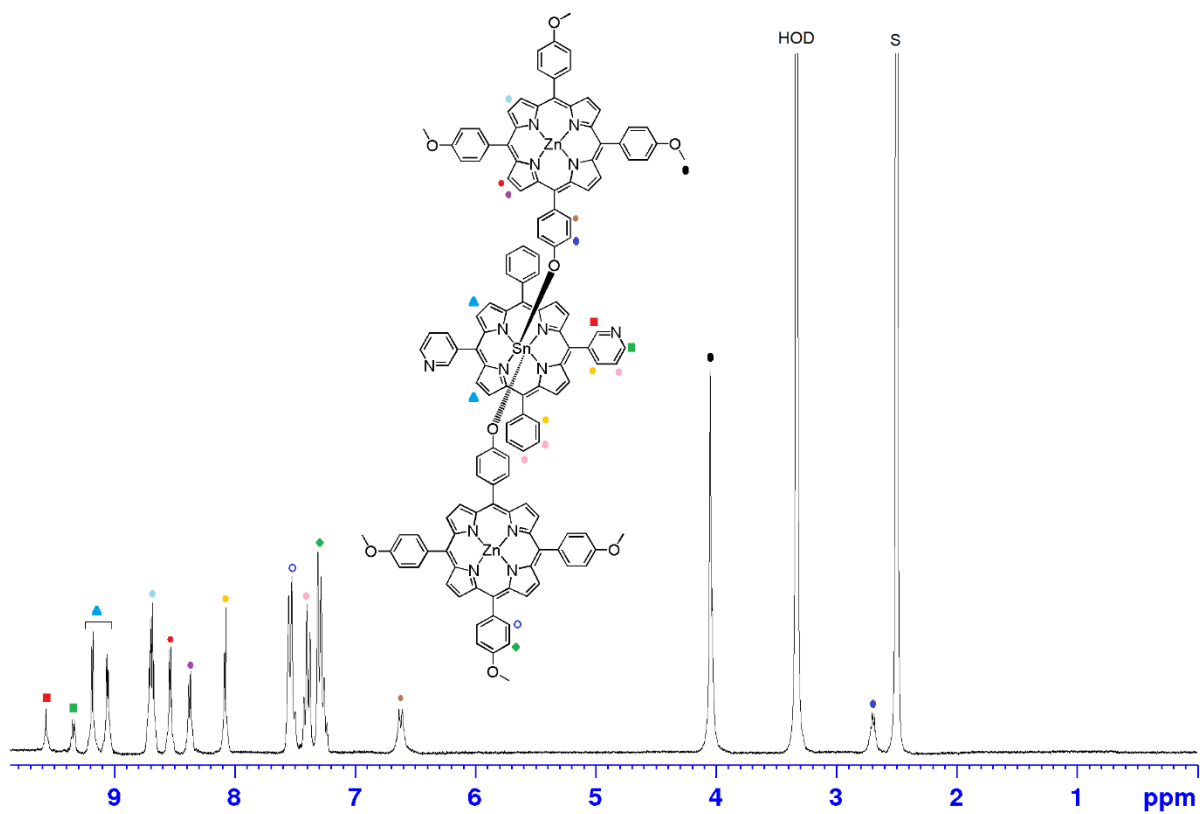


Figure S16. ¹H NMR spectrum of triad **4** in DMSO-d₆.

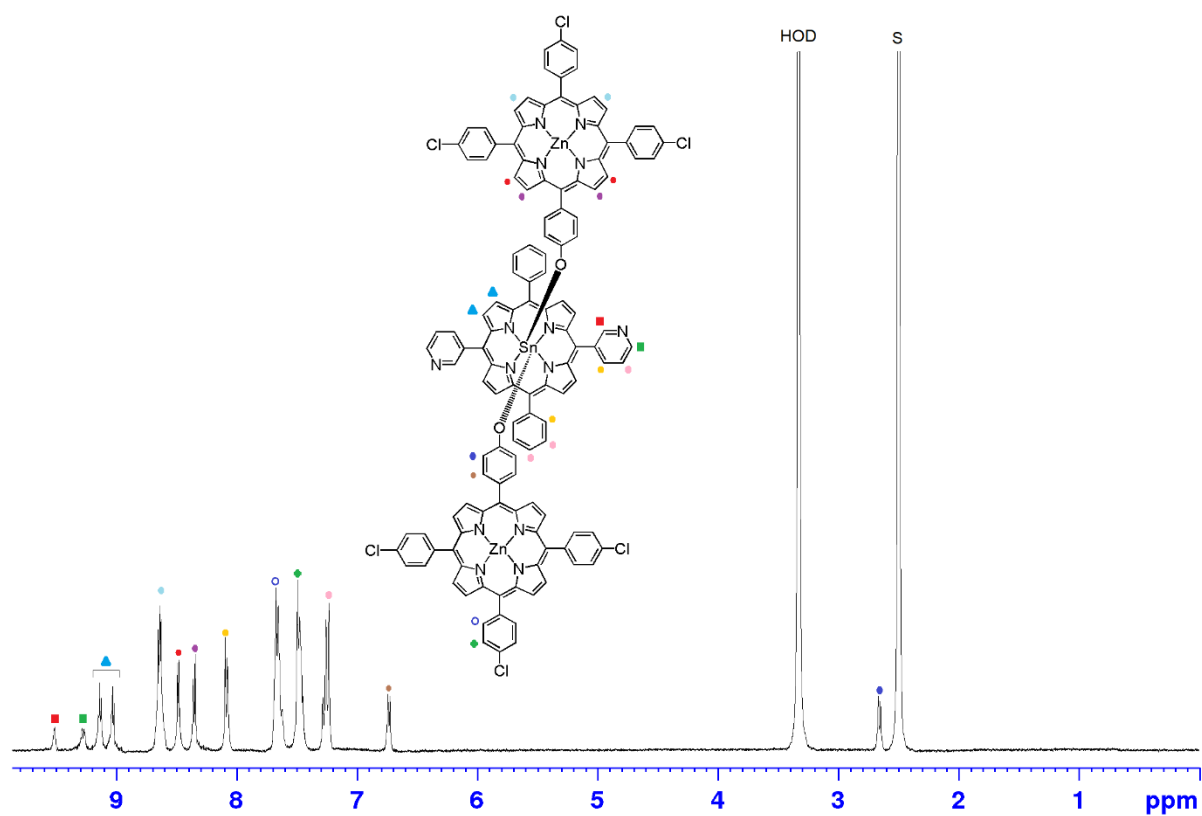


Figure S17. ^1H NMR spectrum of triad **5** in DMSO-d_6 .

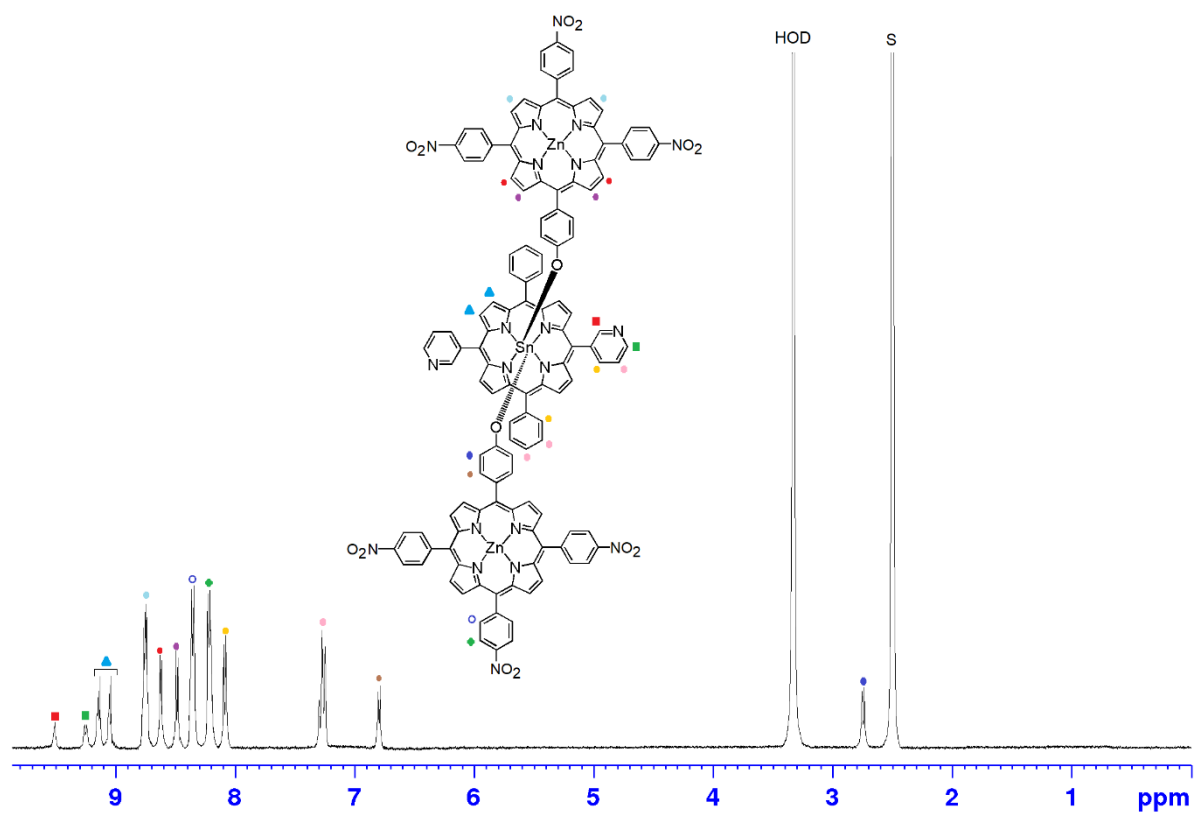


Figure S18. ^1H NMR spectrum of triad **6** in DMSO-d_6 .

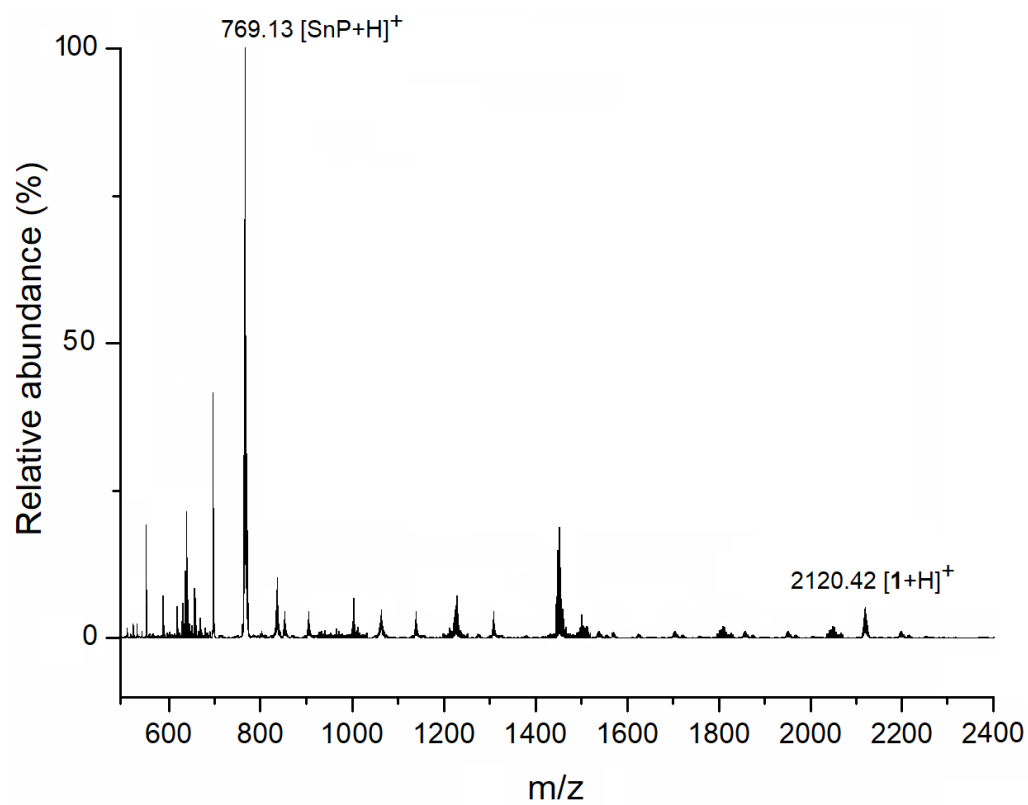


Figure S19. ESI-MS spectrum of triad **1**.

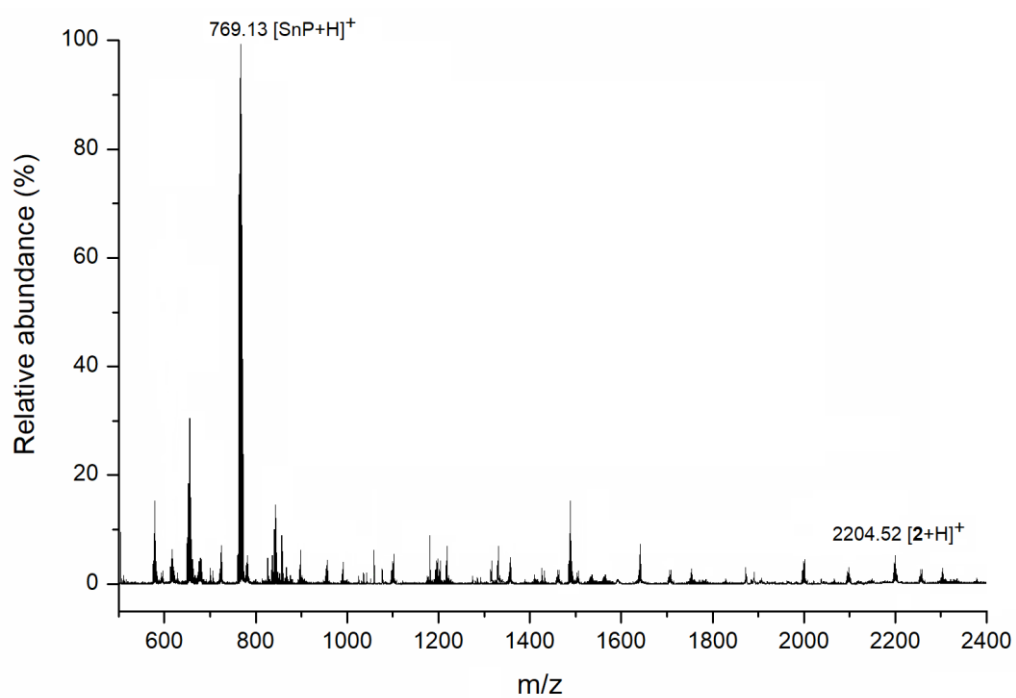


Figure S20. ESI-MS spectrum of triad **2**.

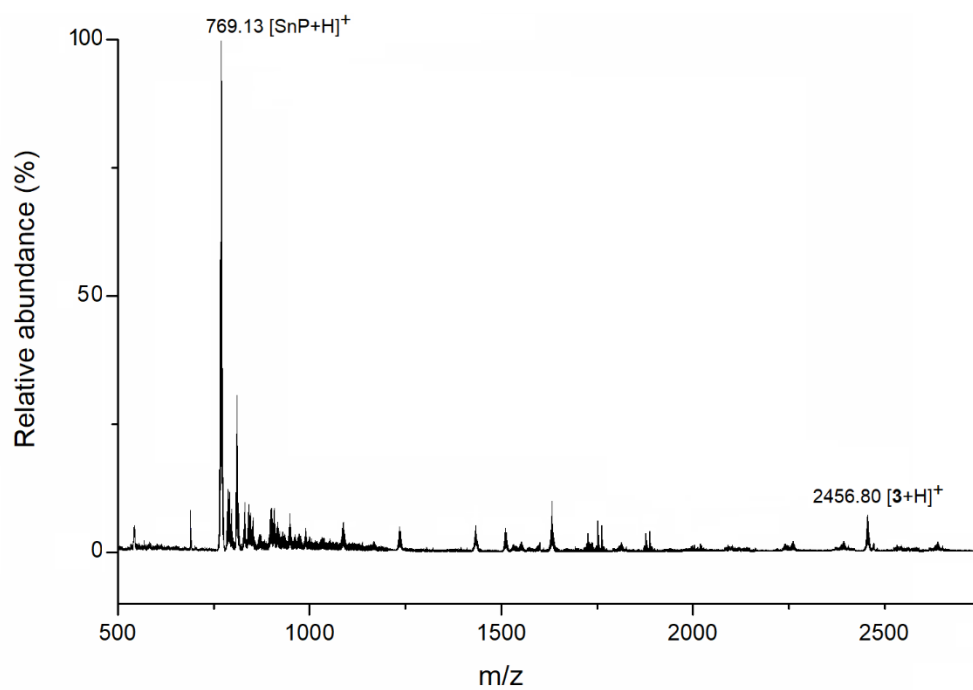


Figure S21. ESI-MS spectrum of triad **3**.

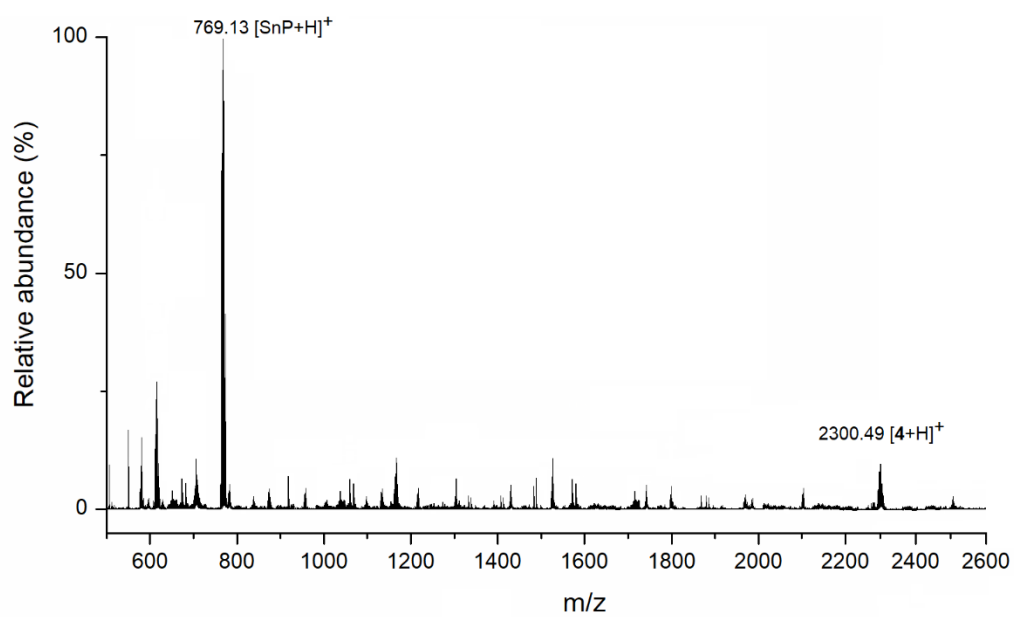


Figure S22. ESI-MS spectrum of triad **4**.

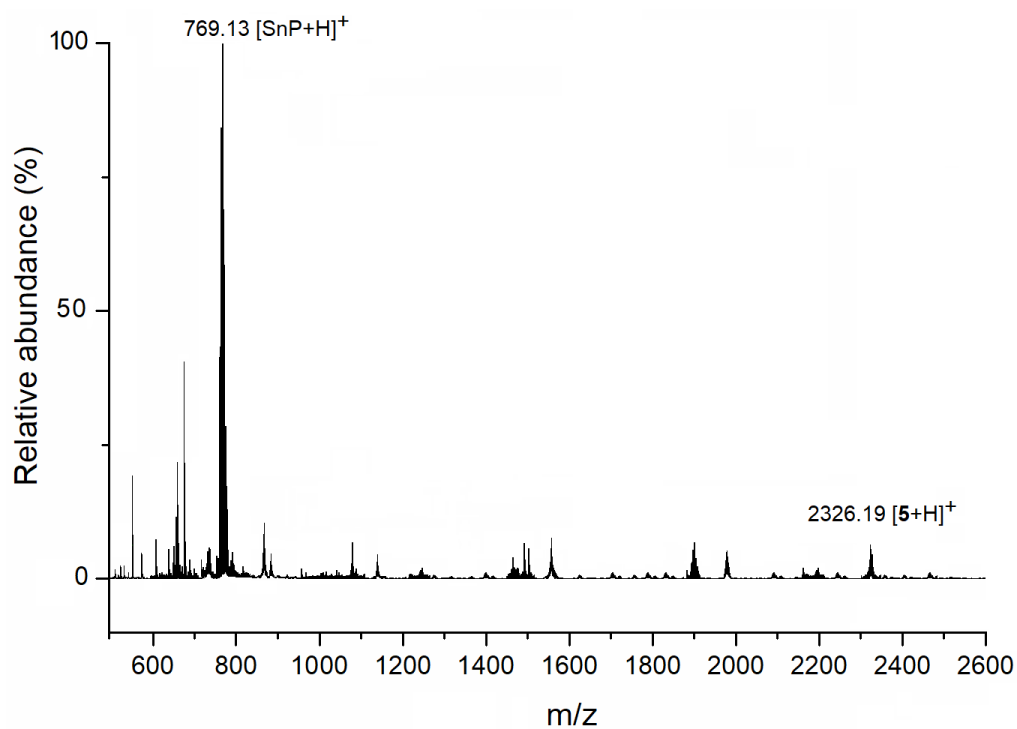


Figure S23. ESI-MS spectrum of triad 5.

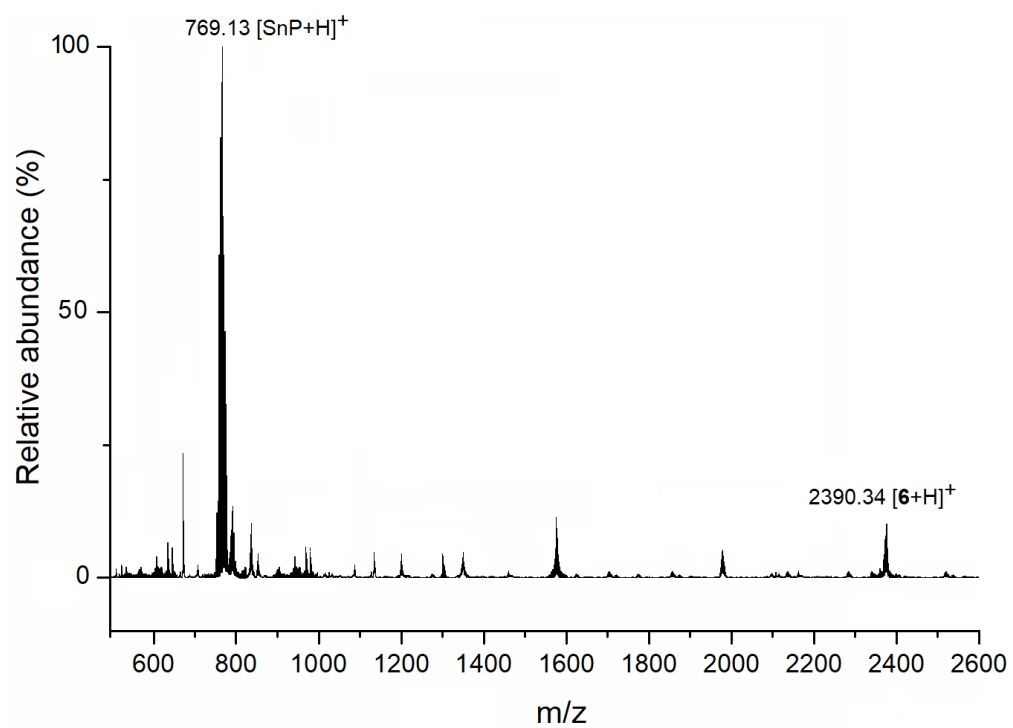


Figure S24. ESI-MS spectrum of triad 6.

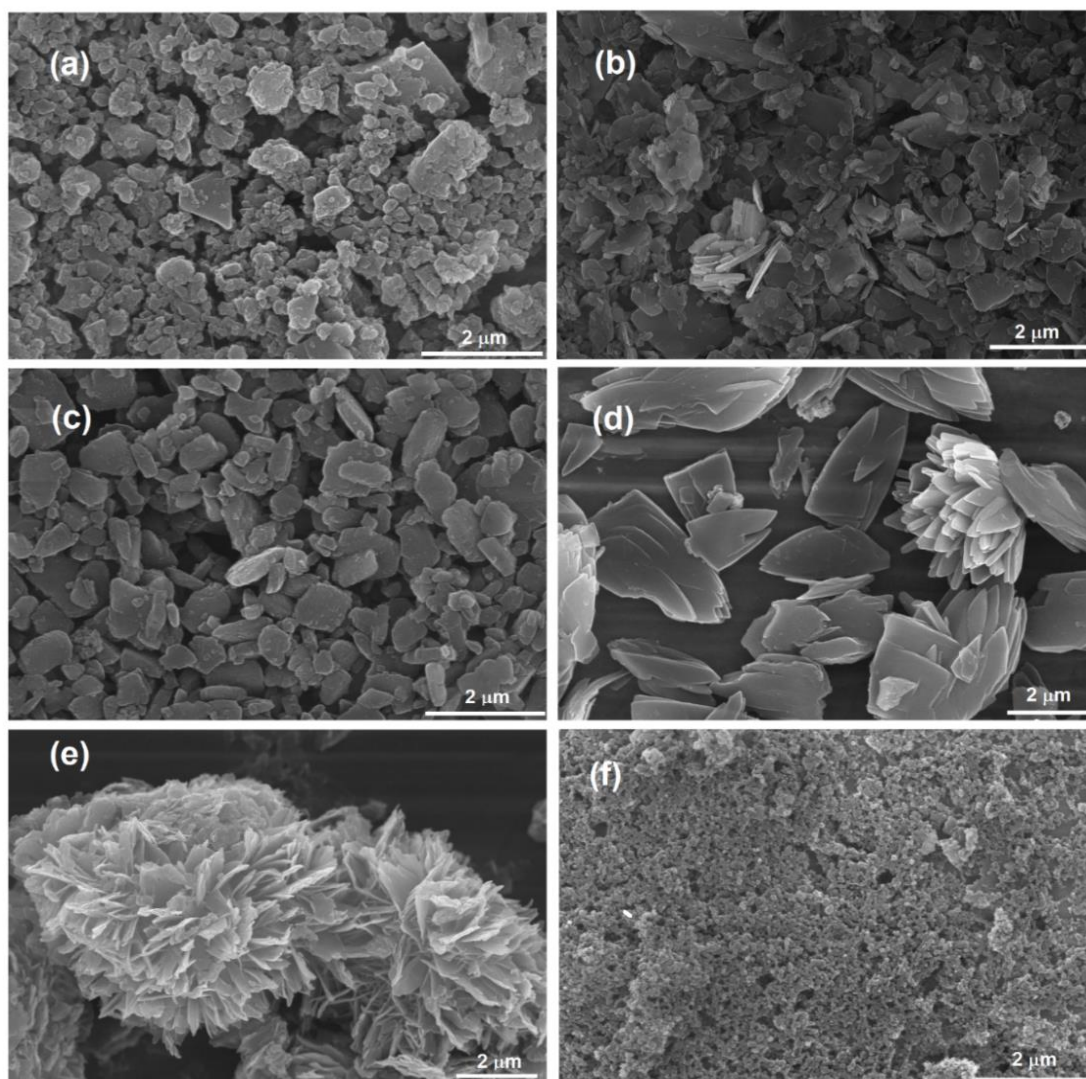


Figure S25. Lower magnification of FE-SEM images for the assembly patterns of triads: (a) **1**; (b) **2**; (c) **3**; (d) **4**; (e) **5**; (f) **6**.

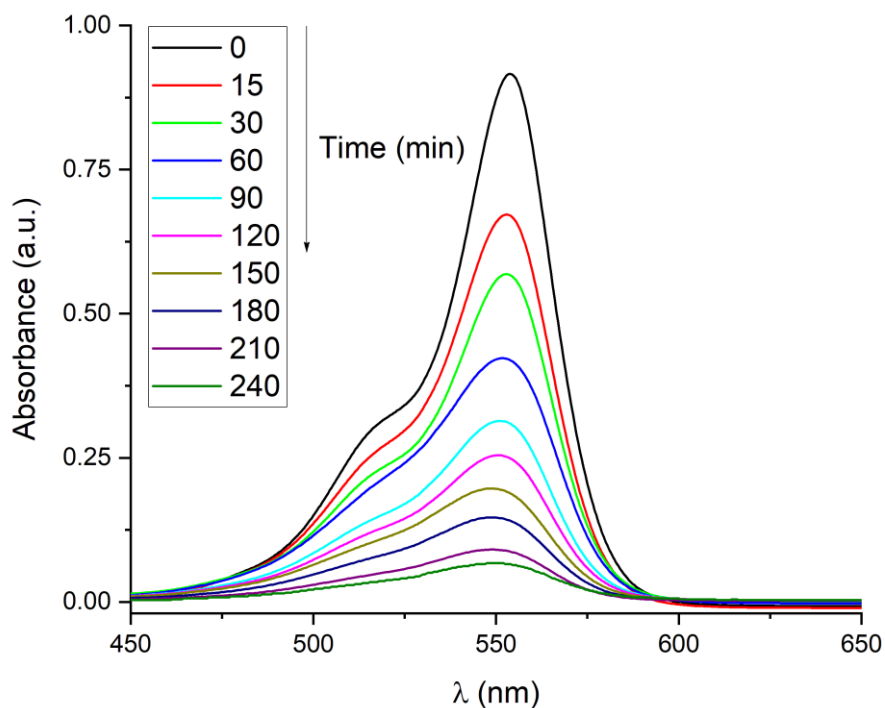


Figure S26. Absorption spectra of RhB in the presence of nano fibers derived from triad **3** under visible light irradiation.

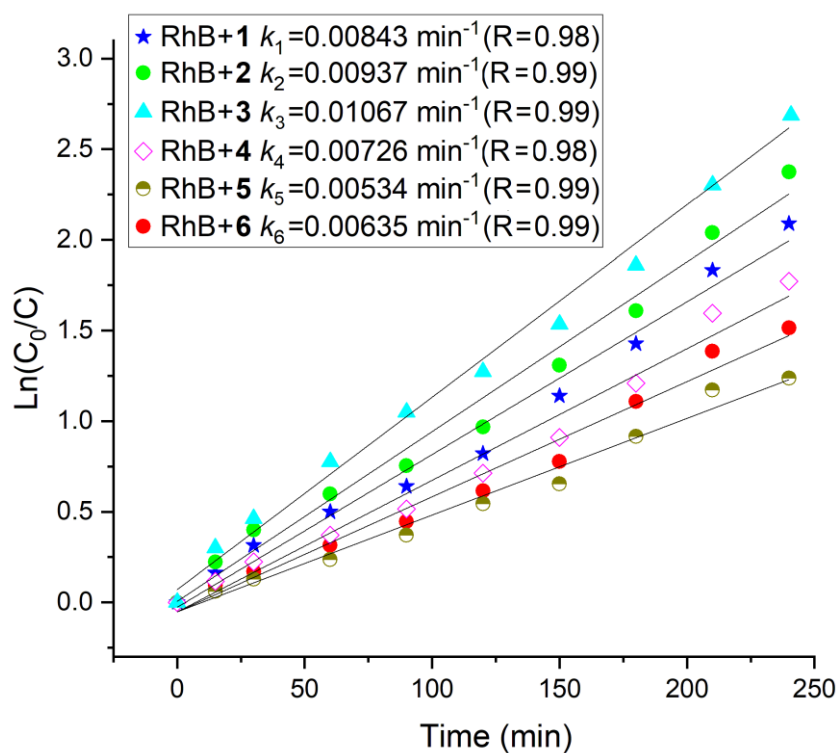


Figure S27. Kinetics for the photocatalytic degradation of RhB under visible light irradiation of the six triads (**1-6**).

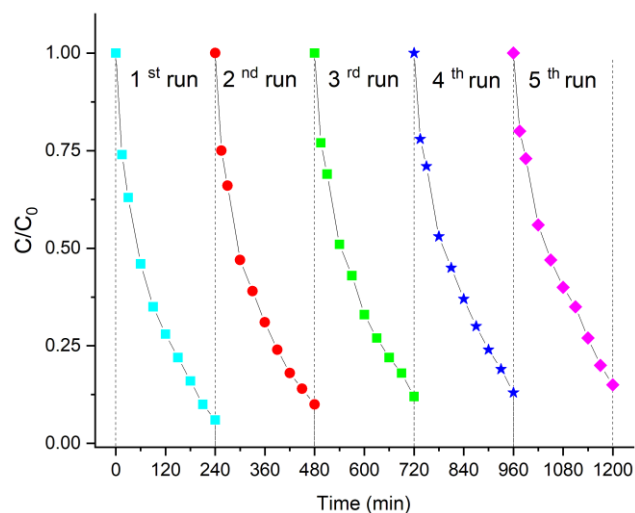


Figure S28. Catalytic cycles (up to 5 cycles) using triad **3** as a photocatalyst for the degradation of RhB.

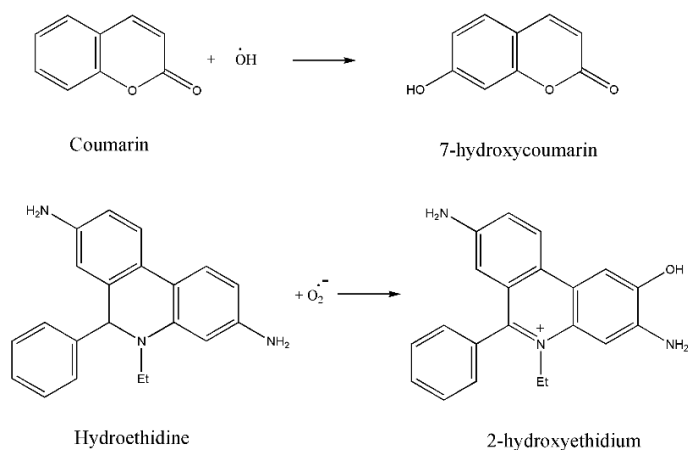


Figure S29. Schematic representation of the detection of the hydroxyl and superoxide radical anion that were generated during the photodegradation experiments.

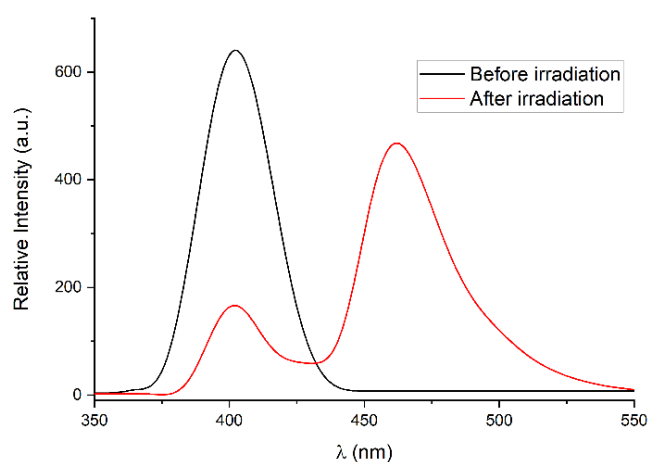


Figure S30. UV-Visible spectra of coumarin in the presence of triad **3** in water. $\lambda_{\text{ex}} = 325$ nm and light exposure time (30 min).